



University of HUDDERSFIELD

University of Huddersfield Repository

Mohammad, Mohammad Amin, Grimsey, Ian M., Forbes, Robert T., Blagbrough, Ian S. and Conway, Barbara R

Effect of mechanical denaturation on surface free energy of protein powders

Original Citation

Mohammad, Mohammad Amin, Grimsey, Ian M., Forbes, Robert T., Blagbrough, Ian S. and Conway, Barbara R (2016) Effect of mechanical denaturation on surface free energy of protein powders. *Colloids and Surfaces B: Biointerfaces*, 146. pp. 700-706. ISSN 0927-7765

This version is available at <http://eprints.hud.ac.uk/id/eprint/29219/>

The University Repository is a digital collection of the research output of the University, available on Open Access. Copyright and Moral Rights for the items on this site are retained by the individual author and/or other copyright owners. Users may access full items free of charge; copies of full text items generally can be reproduced, displayed or performed and given to third parties in any format or medium for personal research or study, educational or not-for-profit purposes without prior permission or charge, provided:

- The authors, title and full bibliographic details is credited in any copy;
- A hyperlink and/or URL is included for the original metadata page; and
- The content is not changed in any way.

For more information, including our policy and submission procedure, please contact the Repository Team at: E.mailbox@hud.ac.uk.

<http://eprints.hud.ac.uk/>

1 **Effect of mechanical denaturation on surface free energy of protein powders**

2 Mohammad Amin Mohammad^{a,b*}, Ian M. Grimsey^a, Robert T. Forbes^a

3 Ian S. Blagbrough^c, and Barbara R Conway^d

4 ^a School of Pharmacy, University of Bradford, Bradford, BD7 1DP, UK.

5 ^b Faculty of Pharmacy, University of Damascus, Damascus, Syria.

6 ^c Department of Pharmacy and Pharmacology, University of Bath, Bath BA2 7AY, UK.

7 ^d Department of Pharmacy, University of Huddersfield, Queensgate, Huddersfield, HD1 3DH,
8 UK.

9
10
11 * Corresponding author

12 Dr. Mohammad Amin Mohammad

13 Associate Professor in Pharmaceutical Technology

14 First name: Mohammad Amin

15 Family name: Mohammad

16 Phone: + 44 (0)1225 386797

17 Email: m.a.mohammad7@bradford.ac.uk

18 Postal address: Dr. Mohammad Amin Mohammad, School of Pharmacy, University of Bradford,
19 Richmond Road, Bradford, BD7 1DP, UK.

20
21 Dr. Ian M. Grimsey, Senior Lecturer in Pharmaceutical Technology

22 Phone: +44 (0)1274 234754

23 Email: i.m.grimsey@bradford.ac.uk

24 School of Pharmacy, University of Bradford, Bradford BD7 1DP, UK

25
26 Prof. Robert T. Forbes, Professor of Biophysical Pharmaceutics

27 Phone: +44 (0)1274 234653

28 Email: r.t.forbes@bradford.ac.uk

29 School of Pharmacy, University of Bradford, Bradford BD7 1DP, UK

30
31 Dr. Ian S. Blagbrough

32 Phone: +44 (0) 1225 386795

33 Email: prsisb@bath.ac.uk

34 Department of Pharmacy and Pharmacology, University of Bath, Bath BA2 7AY, UK.

35
36 Prof. Barbara R Conway,

37 Phone: +44 (0) 1484 472347

38 Email: b.r.conway@hud.ac.uk

39 Department of Pharmacy, University of Huddersfield, Queensgate, Huddersfield, HD1 3DH,
40 UK.

46 **ABSTRACT**

47 Globular proteins are important both as therapeutic agents and excipients. However, their fragile
48 native conformations can be denatured during pharmaceutical processing, leading to
49 modification of the surface energy of their powders and hence their performance. Lyophilized
50 powders of hen egg-white lysozyme and β -galactosidase from *Aspergillus oryzae* were used as
51 models to study the effects of mechanical denaturation on the surface energies of basic and
52 acidic protein powders, respectively. Milling induced mechanical denaturation, confirmed by the
53 absence of any thermal unfolding transition phases and by the changes in their secondary and
54 tertiary structures. Inverse gas chromatography detected differences between both unprocessed
55 protein powders and their denatured forms. The surfaces of the acidic and basic protein powders
56 were relatively basic, however the surface acidity of β -galactosidase was higher than that of
57 lysozyme. Also the surface of β -galactosidase powder had a higher dispersive energy compared
58 to lysozyme. The mechanical denaturation decreased the dispersive energy and the basicity of the
59 surfaces of both protein powders. The amino acid composition and molecular conformation of
60 the proteins explained the surface energy data measured by inverse gas chromatography. The
61 biological activity of mechanically denatured protein powders can either be reversible
62 (lysozyme) or irreversible (β -galactosidase) upon hydration. Our surface data can be exploited to
63 understand and predict the performance of protein powders within pharmaceutical dosage forms.

64

65 *Keywords:*

66 Protein denaturation; β -Galactosidase; Lysozyme; Conformational change; Inverse gas
67 chromatography; Surface free energy.

68 **1. Introduction**

69

70 In the pharmaceutical field, there is considerable interest in the use of globular proteins
71 for their therapeutic effects. During pharmaceutical processes, powders are often subjected to
72 mechanical stresses. For example, milling has been used to prepare protein particles suitable for
73 pulmonary delivery and protein-loaded microparticles in industrial quantities [1,2]. The
74 mechanical stresses applied during the milling process can partially, or completely, denature the
75 proteins and change their bulk properties [3]. In recent years, denatured globular proteins have
76 found extensive applications as excipients in pharmaceutical formulations [4,5]. Denatured
77 globular proteins have been used to prepare emulsion systems designed to enhance the
78 absorption of insoluble drugs and to form nanoparticles for drug delivery and targeting [4].
79 Globular proteins have also been used successfully to formulate controlled drug delivery tablets,
80 which delay drug release in gastric conditions by forming a gel-layer stabilized by
81 intermolecular- β sheets of denatured globular proteins [5].

82 Surface energies of powders are critical properties to be considered during formulation
83 and development of dosage forms in the pharmaceutical industry. Surface energy has significant
84 effects on pharmaceutical processes such as granulation, tableting, disintegration, dissolution,
85 dispersibility, immiscibility, wettability, adhesion, flowability, packing etc. Resultant data from
86 recent determinations of surface energies have been used to reduce the time for formulation
87 development and enhance the quality of the final product [6-8].

88 The effect of denaturation of proteins on their surface chemistry has been determined
89 using time-of-flight secondary ion mass spectrometry [9]. However, the effect of mechanical
90 denaturation on the surface energies of globular proteins has not been reported and these effects
91 must be understood to exploit the full potential of globular proteins in pharmaceutical

92 processing, both as therapeutic agents and excipients. Inverse gas chromatography (IGC) is a
93 useful verified tool for surface energy measurements [10]. IGC has been used to measure the
94 surface free energy of lyophilized protein particles, detecting lot-to-lot variations in the
95 amorphous microstructure of lyophilized protein formulations [11].

96 This study aims to evaluate the effects of mechanical denaturation on the surface energies
97 of globular protein powders using IGC. β -Galactosidase is a hydrolytic enzyme that has been
98 widely investigated for potential applications in the food industry to improve sweetness,
99 solubility, flavor, and digestibility of dairy products. Preparations of β -galactosidases have also
100 been exploited for industrial, biotechnological, medical, and analytical applications [12].
101 Lysozyme is a naturally occurring enzyme found in bodily secretions such as tears, saliva, and
102 milk and has been explored as a food preservative and pharmaceutical. The isoelectric points (pI)
103 of β -galactosidase (from *Aspergillus oryzae*) and hen egg-white lysozyme are 4.6 and 11.3, and
104 were used as models of acidic and basic globular proteins, respectively [13]. Lyophilized
105 powders of these proteins were mechanically denatured by milling. Their surface energies before
106 and after denaturation were compared in order to understand how the surfaces of the globular
107 protein powders were affected by the denaturation process.

108

109 **2. Materials and methods**

110 *2.1. Materials*

111 *Micrococcus lysodeikticus* (Sigma-Aldrich) and 2-nitrophenyl β -D-galacto pyranoside
112 (Sigma-Aldrich), lyophilized powders of β -galactosidase from *A. oryzae* (Sigma-Aldrich) and
113 hen egg-white lysozyme (Biozyme Laboratories, UK) were purchased as indicated. The

114 purchased β -galactosidase and lysozyme powders were designated as unprocessed samples and
115 named UNG and UNL, respectively.

116

117 *2.2. Preparation of mechanically denatured protein powders*

118 Mechanically denatured powders of β -galactosidase and lysozyme were prepared by
119 manually milling. The milling was achieved by rotating a marble pestle over the powder within a
120 marble mortar at ~45 cycles per minute (cpm). Milling durations of 60 min were enough to
121 completely denature the protein powders, and this was confirmed by differential scanning
122 calorimetry (DSC) [3]. The mechanically denatured powders of β -galactosidase and lysozyme
123 were named DeG and DeL, respectively. Three batches (2 g each batch) of the mechanically
124 denatured powders were prepared for each protein.

125

126 *2.3. Microscopy*

127 A Zeiss Axioplan2 polarizing microscope (Carl Zeiss Vision GmbH; Hallbergmoos,
128 Germany) was used to visualize the samples. The accompanying software (Axio Vision 4.2) was
129 then used to determine the projected area diameters of the powders.

130

131 *2.4. Differential scanning calorimetry (DSC)*

132 Differential scanning calorimetry (DSC) thermograms were obtained using a Perkin-
133 Elmer Series 7 DSC (Perkin-Elmer Ltd., Beaconsfield, UK). Samples (4-7 mg) were sealed in
134 aluminium pans. The escape of water was facilitated by making a pinhole in the lid prior to
135 sealing. The samples were equilibrated at 25 °C and heated to 250 °C at a scan heating rate of 10
136 °C/min under a flow of anhydrous nitrogen (20 ml/min). Each sample was analysed in triplicate.

137 The temperature axis and cell constant of the DSC cell were calibrated with indium (10 mg,
138 99.999 % pure, melting point 156.60 °C, and heat of fusion 28.40 J/g).

139

140 2.5. FT-Raman spectroscopy

141 FT-Raman spectra of samples were recorded with a Bruker IFS66 optics system using a
142 Bruker FRA 106 Raman module. The excitation source was an Nd: YAG laser operating at 1064
143 nm and a laser power of 50 mW was used. The FT-Raman module was equipped with a liquid
144 nitrogen-cooled germanium diode detector with an extended spectrum band width covering the
145 wave number range 1800-450 cm^{-1} . Samples were placed in stainless steel sample cups and
146 scanned 200 times with the resolution set at 8 cm^{-1} . The observed band wave numbers were
147 calibrated against the internal laser frequency and are correct to better than $\pm 1 \text{ cm}^{-1}$. The spectra
148 were corrected for instrument response. The experiments were run at a controlled room
149 temperature of $20 \pm 1 \text{ }^\circ\text{C}$.

150

151 2.6. Enzymatic assay

152 The enzymatic activity of lysozyme samples was measured to determine the ability of
153 lysozyme to catalyze the hydrolysis of β -1,4-glycosidic linkages of cell-wall
154 mucopolysaccharides [14]. Lysozyme solution (30 μl , 0.05 % in phosphate buffer, pH = 5.2; 10
155 mM) was added to *Micrococcus lysodeikticus* suspension (2.97 ml, 0.025 % in phosphate buffer,
156 pH = 6.24; 66 mM). The decrease in the absorbance at 450 nm was monitored UV-Vis
157 spectrophotometry (PU 8700, Philips, UK). The activity was determined by measuring the
158 decrease in the substrate bacterial suspension concentration with time. Hence the slope of the
159 reduction in light absorbance at 450 nm against the time of 3 min, starting when the protein

160 solutions were mixed with the substrate bacterial suspension, was considered to be the indicator
161 of the lytic activity of lysozyme [15].

162 The enzymatic activity of β -galactosidase samples was determined using a method
163 relying on the ability of β -galactosidase to hydrolyse the chromogenic substrate *o*-nitrophenyl β -
164 D-galacto pyranoside (ONPG) to *o*-nitrophenol [16]. The results were achieved by adding 20 μ l
165 of protein solution (0.05 w/v% in deionised water) to 4 ml of the substrate solution (0.665
166 mg/ml) in a phosphate buffer (100 mM and pH = 7). The mixture then was incubated for 10 min
167 in a water bath at 30 ± 1 °C. The absorbance at 420 nm was used to indicate the activity.

168 The concentrations of the protein solutions had been determined prior to the activity tests
169 using the following equation:

$$170 \quad [Protein] = Abs_{280 \text{ nm}}/E_{280 \text{ nm}} \quad (1)$$

171 where $[Protein]$ is the concentration of protein in the tested solution w/v%, $Abs_{280 \text{ nm}}$ is the
172 absorbance of the tested protein solution at 280 nm and $E_{280 \text{ nm}}$ is the absorbance of protein
173 standard solution with concentration 0.05 w/v%. The solutions were diluted to about 0.05 % w/v
174 (to produce absorbances <0.8). The activities of all samples were measured relative to that of a
175 corresponding fresh sample, which was considered as the standard solution.

176

177 2.7. Inverse gas chromatography

178 IGC experiments were performed using an inverse gas chromatography (IGC 2000,
179 Surface Measurement Systems Ltd., UK). A sample (~500 mg) was packed into a pre-silanised
180 glass column (300 mm \times 3 mm i.d.). Three columns of each sample were analysed at 30 °C (the

181 lowest temperature at which the IGC experiments can be performed to avoid thermal stress) and
182 zero relative humidity, using anhydrous helium gas as the carrier. A series of n-alkanes (n-
183 hexane to n-nonane) in addition to chloroform, as a monopolar electron acceptor probe (l_+), and
184 ethyl acetate, as a monopolar donor acceptor probe (l_-), were injected through the columns at the
185 infinite dilution region. Their retention times followed from detection using a flame ionization
186 detector (FID).

187

188 2.7.1. Surface energy calculations

189 Our published methods were used to calculate the surface energies and verify their
190 accuracy [17-19]. These methods describe the surface properties using the dispersive retention
191 factor ($K_{CH_2}^a$), the electron acceptor retention factor ($K_{l_+}^a$), and the electron donor retention factor
192 ($K_{l_-}^a$), which are calculated using the retention times of probes:

$$193 \quad \ln(t_r - t_0) = (\ln K_{CH_2}^a) n + C \quad (2)$$

194 where n is the carbon number of the homologous n-alkanes, t_r and t_0 are the retention times of
195 the n-alkanes and a non-adsorbing marker, respectively, $K_{CH_2}^a$ is the dispersive retention factor of
196 the analysed powder and C is a constant. The linear regression statistics of equation 2 generate
197 the value of t_0 which gives its best linear fit. The slope of the equation 2 gives the value of $K_{CH_2}^a$.

$$198 \quad K_{l_+}^a = t_{nl+} / t_{nl+,ref} \quad (3)$$

$$199 \quad K_{l_-}^a = t_{nl-} / t_{nl-,ref} \quad (4)$$

200 where t_{nl+} and $t_{nl+,ref}$ are the retention time of l_+ and its theoretical n-alkane reference,
201 respectively, t_{nl-} and $t_{nl-,ref}$ are the retention time of l_- and its theoretical n-alkane reference,
202 respectively.

203
$$\ln t_{nl+,ref} = \ln t_{nCi} + \left(\frac{\alpha_{l+}(\gamma_{l+}^d)^{0.5} - \alpha_{Ci}(\gamma_{Ci}^d)^{0.5}}{\alpha_{CH_2}(\gamma_{CH_2})^{0.5}} \right) \ln K_{CH_2}^a \quad (5)$$

204
$$\ln t_{nl-,ref} = \ln t_{nCi} + \left(\frac{\alpha_{l-}(\gamma_{l-}^d)^{0.5} - \alpha_{Ci}(\gamma_{Ci}^d)^{0.5}}{\alpha_{CH_2}(\gamma_{CH_2})^{0.5}} \right) \ln K_{CH_2}^a \quad (6)$$

205 where α_{CH_2} and γ_{CH_2} , α_{Ci} and γ_{Ci}^d , α_{l+} and γ_{l+}^d , and α_{l-} and γ_{l-}^d are the cross-sectional area and
 206 the dispersive free energy of a methylene group, an n-alkane, l_+ and l_- , respectively. t_{nCi} is the
 207 retention time of the n-alkane.

208 The retention factors are then used to calculate the surface dispersive (γ_s^d), electron donor (γ_s^-)
 209 and electron acceptor (γ_s^+) components of the powders:

210
$$\gamma_s^d = \frac{0.477 (T \ln K_{CH_2}^a)^2}{(\alpha_{CH_2})^2 \gamma_{CH_2}} \text{ mJ.m}^{-2} \quad (7)$$

211
$$\gamma_s^- = \frac{0.477 (T \ln K_{l+}^a)^2}{(\alpha_{l+})^2 \gamma_{l+}^+} \text{ mJ.m}^{-2} \quad (8)$$

212
$$\gamma_s^+ = \frac{0.477 (T \ln K_{l-}^a)^2}{(\alpha_{l-})^2 \gamma_{l-}^-} \text{ mJ.m}^{-2} \quad (9)$$

213 where γ_{l+}^+ is the electron acceptor component of l_+ and γ_{l-}^- is the electron donor component of
 214 l_- . The units of α are \AA^2 and of γ are mJ.m^{-2} in all equations.

215 The parameters of CH_2 are calculated from the following equation:

216
$$(\alpha_{CH_2})^2 \gamma_{CH_2} = -1.869T + 1867.194 \text{ \AA}^4 \cdot \text{mJ.m}^{-2} \quad (10)$$

217 The parameters of polar probes are still under debate and different values have been
 218 reported [20-25]. In this paper, we used the values which were recently used for ethyl acetate
 219 ($\gamma_{l-}^- = 19.20 \text{ mJ/m}^2$, $\gamma_{l-}^d = 19.60 \text{ mJ/m}^2$, $\alpha_{l-} = 48.0 \text{ \AA}^2$) and for chloroform ($\gamma_{l+}^+ = 3.80 \text{ mJ/m}^2$,
 220 $\gamma_{l+}^d = 25.90 \text{ mJ/m}^2$, $\alpha_{l+} = 44.0 \text{ \AA}^2$) [17,22]. However, using any other different reported numbers
 221 will not change the findings of the comparison.

222 The percentage coefficient of variation of $\ln K_{CH_2}^a$ ($\%CV_{\ln K_{CH_2}^a}$) is an indicator of the
 223 accuracy of the surface energy measurements. The error of the slope of the equation 2
 224 ($SD_{\ln K_{CH_2}^a}$) is used to calculate $\%CV_{\ln K_{CH_2}^a}$:

$$225 \quad \%CV_{\ln K_{CH_2}^a} = \left(SD_{\ln K_{CH_2}^a} / \ln K_{CH_2}^a \right) \times 100 \quad (11)$$

226 $\%CV_{\ln K_{CH_2}^a}$ should be less than 0.7% to accept the accuracy of the measurement. $\%CV_{\ln K_{CH_2}^a}$ is then
 227 used to calculate the uncertainty range of γ_s^d :

$$228 \quad \text{Uncertainty Range of } \gamma_s^d = \left[\left(\frac{100 \times \gamma_s^d}{100 + 7.5\% CV_{\ln K_{CH_2}^a}} \right) \text{ to } \left(\frac{100 \times \gamma_s^d}{100 - 7.5\% CV_{\ln K_{CH_2}^a}} \right) \right] \quad (12)$$

229

230 3. Results and discussion

231 3.1. Microscopy

232 The photomicrographs of UNL, UNG, DeL, and DeG powders show that they had
 233 projected area diameters of $\sim 4 \mu\text{m}$ (Fig. S1), $\sim 2.5 \mu\text{m}$ (Fig. S2), $\sim 1.5 \mu\text{m}$ (Fig. S3), and $\sim 1.5 \mu\text{m}$
 234 (Fig. S4), respectively. The particle sizes of the original powders were below $5 \mu\text{m}$. Therefore,
 235 the attrition mechanism was dominant during milling, and so the same original faces did not
 236 change [3].

237

238 3.2. Differential scanning calorimetry (DSC)

239 For both proteins, DSC thermograms exhibited broad peaks ranging from ~ 30 to $\sim 140 \text{ }^\circ\text{C}$
 240 (Figure 1). These peaks are due to water removal, and their areas depend on water residues in the
 241 powders [3]. The enthalpy of the water evaporation peak was 118 ± 11 , 124 ± 6 , 114 ± 9 and 130 ± 8
 242 J/g for UNL, UNG, DeL, and DeG, respectively, and did not significantly change after milling (t-

243 test: $P < 0.05$). The proteins exchange water with the surrounding air depending on the relative
244 temperature, humidity and exposure time. Therefore, the conditions used in this study did not
245 induce water content change in the milled powders. Also Figure 1 shows that the unprocessed
246 proteins unfolded and a peak was detected at their apparent denaturation temperatures, which
247 varied according to the protein. DSC thermograms of UNL displayed one denaturation peak at
248 ~ 201 °C, but UNG displayed two denaturation peaks at ~ 176 °C and ~ 212 °C.
249

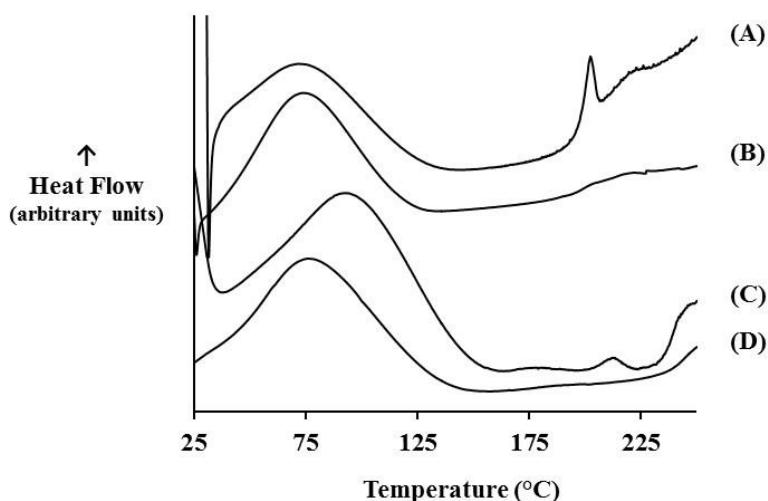


Fig. 1. Example DSC thermograms of protein powders (A) unprocessed lysozyme, (B) mechanically denatured lysozyme, (C) unprocessed β -galactosidase, (D) mechanically denatured β -galactosidase. Conditions: samples heated from 25 to 250 °C; heating rate: 10 °C/min.

250

251 The difference in the thermal denaturation pattern can be due to the difference in the
252 thermal unfolding mechanisms of the proteins. While lysozyme folds in a highly cooperative
253 manner and so exhibits an all-or-none thermal unfolding transition, β -galactosidase goes through
254 a non-two state thermal unfolding transition resulting in two peaks [26,27]. The unfolding
255 transition peaks were completely lost after mechanical denaturation. Hence there was no peak at

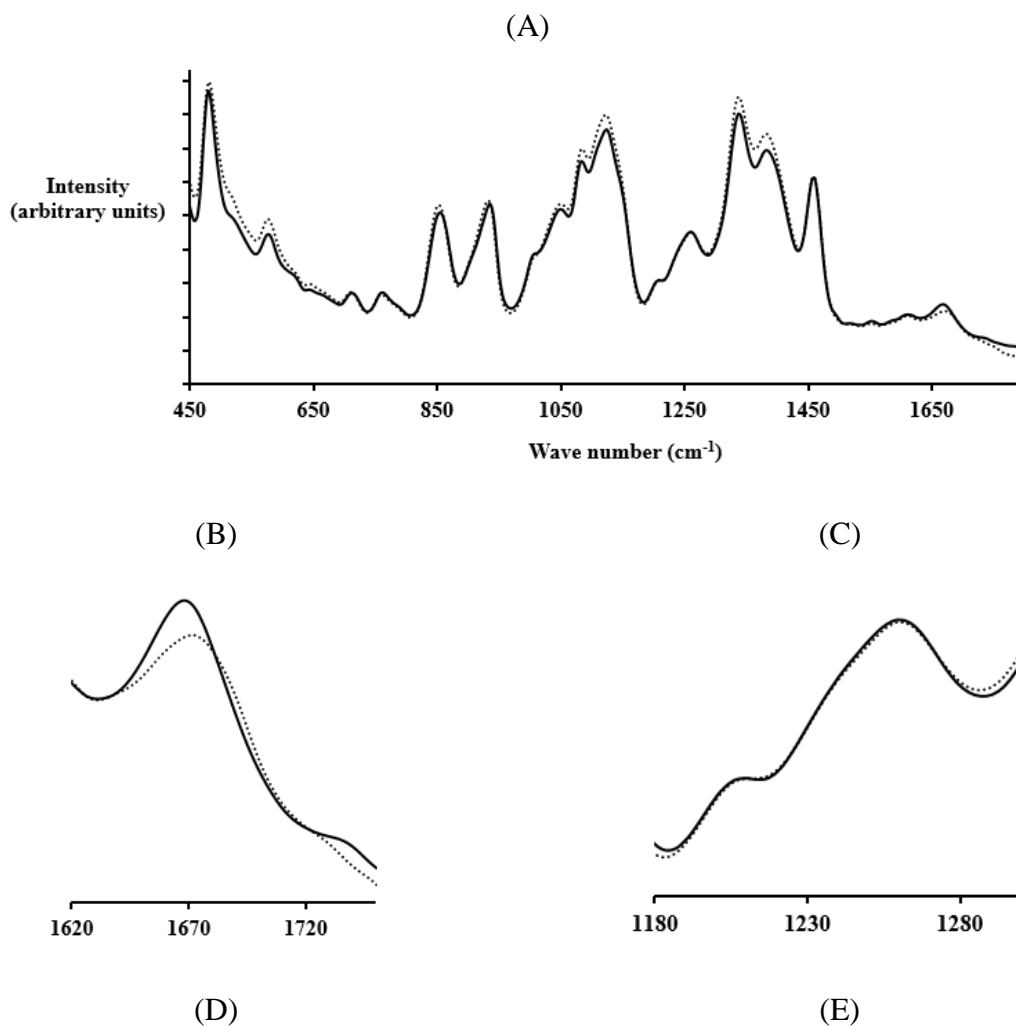
256 ~201 °C for the milled lysozyme samples and neither were there peaks at ~176 °C and ~212 °C
257 for milled β -galactosidase. The complete disappearance of the unfolding transition peak from the
258 DSC thermogram indicates the total transition of the protein from its folded state to its unfolded
259 state [3].

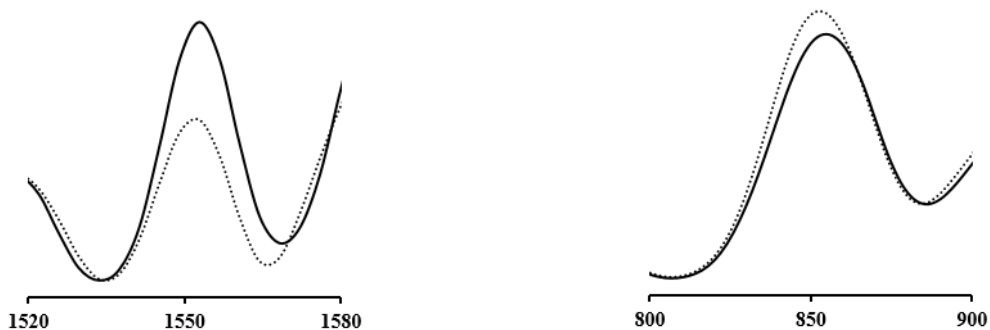
260

261 3.3. FT-Raman study

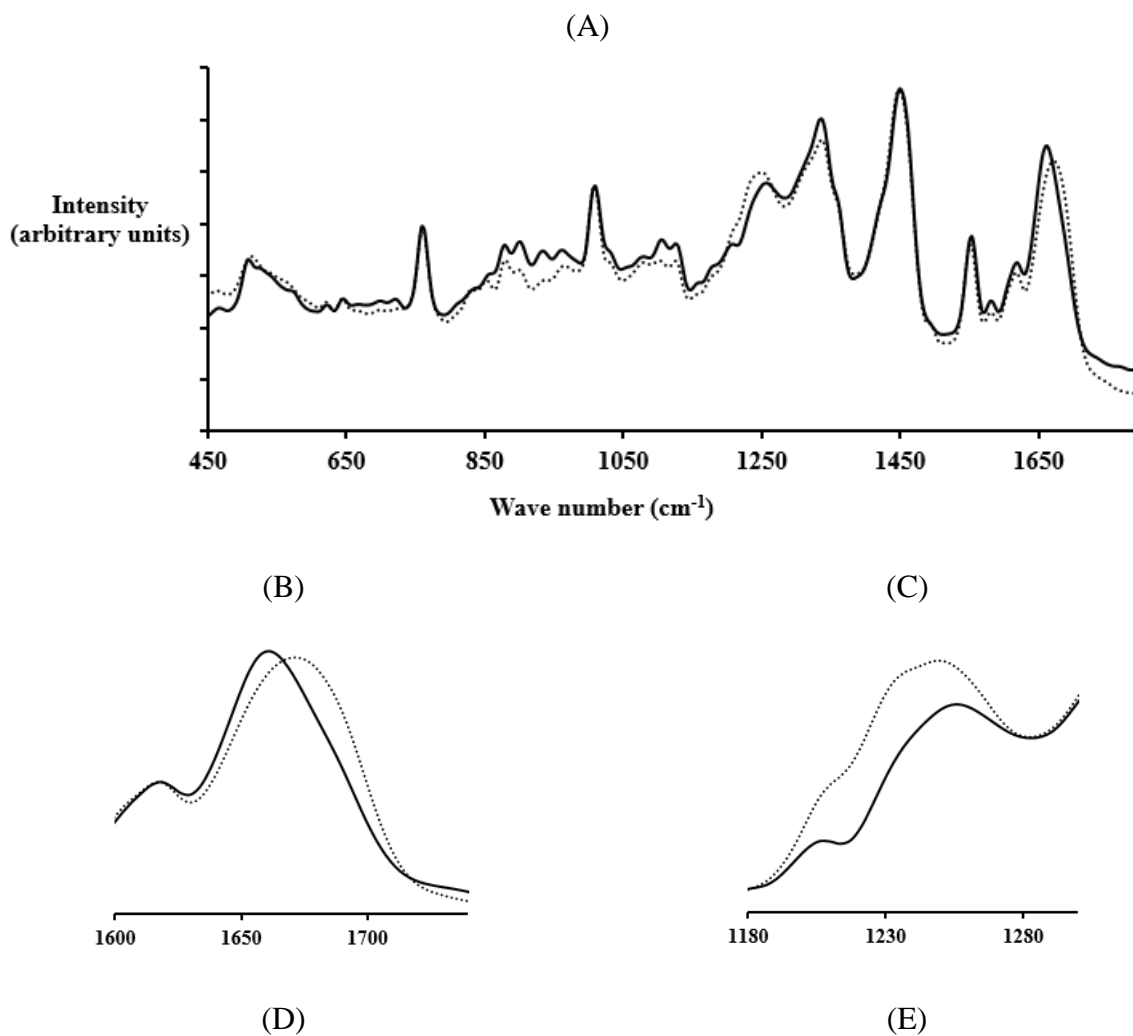
262 Raman spectroscopy was used to compare the molecular conformation of protein
263 powders before and after mechanical denaturation. The band at $\sim 1450\text{ cm}^{-1}$ indicates the CH
264 bending vibrations of aliphatic side chains, and its intensity and position are unaffected by
265 changes induced in protein structure after dehydration or applying different stresses [28].
266 Therefore, it was used as an internal intensity standard to normalize Raman spectra before
267 comparison (Figures 2A and 3A). The vibration modes of amide I (C=O stretch) from 1580 to
268 1720 cm^{-1} (Figures 2B and 3B) and amide III (N-H in-plane bend + C-N stretch) from 1250–
269 1330 cm^{-1} (Figures 2C and 3C) demonstrated the secondary structure of β -galactosidase and
270 lysozyme, respectively. The spectra of the denatured samples show that the modes of the amide I
271 upshifted and broadened for both proteins, and the mode of the amide III intensified and
272 downshifted, especially for lysozyme, but there was no change in the mode of amide III for β -
273 galactosidase. These changes indicated the transformation of α -helix content to β -sheets or a
274 disordered structure which enhances the tendency of proteins to aggregate [3,29]. While β -
275 galactosidase is a beta-type protein, containing mainly β -sheet structure and only 5% α -helix
276 [30], the secondary structure of lysozyme consists of 30% α -helix [31]. This explains why no
277 changes in the amide III of β -galactosidase were observed.

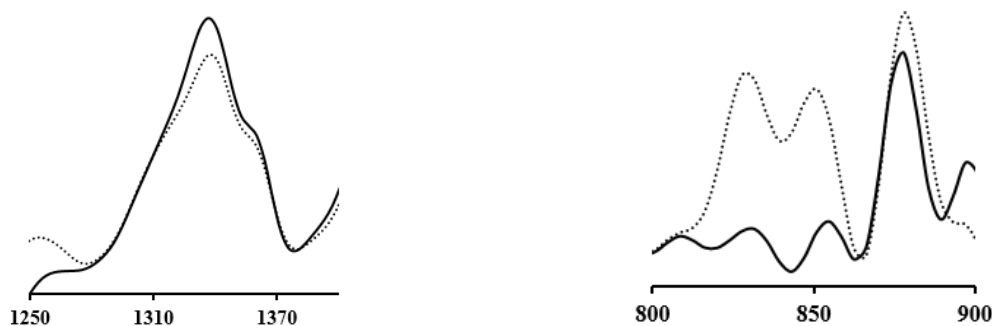
278 The aggregation of denatured proteins, combined with changes in the vibration modes of
279 the aromatic residues at $\sim 1550\text{ cm}^{-1}$ in β -galactosidase (Figure 2D), $1320\text{-}1380\text{ cm}^{-1}$ in lysozyme
280 (Figure 3D) and $800\text{-}900\text{ cm}^{-1}$ in both proteins (Figures 2E and 3E). These changes in the
281 vibration modes of the aromatic residues result from the changes in their micro-environment
282 after denaturation because of their roles in the denaturation processes [29,32]. The aggregates of
283 denatured protein molecules are formed via π -stacking interactions of the aromatic residues [33].





284 **Fig. 2.** FT-Raman spectra of β -galactosidase powders, the unprocessed powders (solid lines) and
 285 the mechanically denatured powders (dotted lines). Vibration modes of secondary structure are
 286 (B) amide I and (C) amide III. Vibration modes of tertiary structure are (D) for Trp and (E) for
 287 Trp and Tyr. The spectra were normalized using the methylene deformation mode at $\sim 1450\text{ cm}^{-1}$
 288 as an internal intensity standard.
 289





290 **Fig. 3.** FT-Raman spectra of lysozyme powders, the unprocessed powders (solid lines) and the
 291 mechanically denatured powders (dotted lines). Vibration modes of secondary structure are (B)
 292 amide I and (C) amide III. Vibration modes of tertiary structure are (D) for Trp and (E) for Trp
 293 and Tyr. The spectra were normalized using the methylene deformation mode at $\sim 1450\text{ cm}^{-1}$ as
 294 an internal intensity standard.
 295

296 3.4. Enzymatic assay

297 Therapeutic proteins may rapidly denature and lose their enzymatic activity. The
 298 structural changes detected using FT-Raman and the absence of any T_m by DSC have been used
 299 to monitor the denaturation of proteins, and the results of Raman and DSC are linked to the
 300 results of enzymatic activity [34]. Our DSC and Raman results confirmed the denaturation of
 301 both proteins studied. The enzymatic assay showed that the mechanically denatured β -
 302 galactosidase samples demonstrated no enzymatic activity (Figure 4). However, the
 303 mechanically denatured lysozyme samples maintained full enzymatic activity when compared to
 304 an unprocessed sample (t-test: $P < 0.05$) (Figure 4). This is due to the ability of denatured
 305 lysozyme to refold upon dissolution in aqueous media and thus the biological activity of
 306 lysozyme is fully recovered following dissolution [3.35].
 307

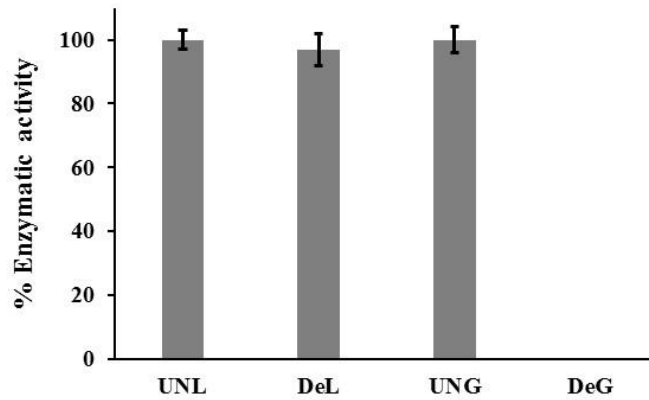


Fig. 4. Enzymatic activity of the unprocessed powders and the mechanically denatured powders of lysozyme and β -galactosidase.

3.5. Surface free energy

The IGC results (Table 1) confirm the acceptable accuracy of the IGC experiments considered in this work with $\%CV_{\ln K_{CH_2}^a}$ values of less than 0.7% [18]. IGC data for the unprocessed powders demonstrated the differences in the surface free energy between β -galactosidase (an acidic protein) and lysozyme (a basic protein). UNG had higher γ_s^d compared to UNL because the uncertainty ranges of γ_s^d of UNG and UNL did not overlap for the three columns [18]. The surface acidity (γ_s^+) and the surface basicity (γ_s^-) of UNG were significantly different from UNL (t-test: $P < 0.05$). The average of γ_s^+ was 16.2 ± 0.2 and 12.4 ± 0.1 $\text{mJ} \cdot \text{m}^{-2}$ and the average of γ_s^- was 5.5 ± 0.2 and 10.5 ± 0.6 $\text{mJ} \cdot \text{m}^{-2}$ for UNG and UNL, respectively. This proves that UNG, chosen as a model for acidic proteins, has higher surface acidity and lower surface basicity compared to selected basic protein, UNL.

Table 1. The surface energies (γ_s^d , γ_s^+ and γ_s^-) and retention factors ($K_{CH_2}^a$, K_{l+}^a and K_{l-}^a) of the lyophilized lysozyme powder (UNL), the lyophilized β -galactosidase powder (UNG), the

326 mechanically denatured lyophilized lysozyme powder (DeL) and the mechanically denatured
 327 lyophilized β -galactosidase powder (DeG).

Material	Column	$K_{CH_2}^a$	K_{l+}^a	K_{l-}^a	$\%CV_{\ln K_{CH_2}^a}$	γ_s^d mJ.m ⁻²	Uncertainty Range of γ_s^d mJ.m ⁻²	γ_s^+ mJ.m ⁻²	γ_s^- mJ.m ⁻²
UNL	1	3.099	3.725	34.572	0.144	43.1	41.9-44.4	12.4	10.3
UNL	2	3.095	3.677	34.668	0.094	43.0	42.2-43.9	12.5	10.1
UNL	3	3.089	3.944	33.704	0.077	42.9	42.2-43.6	12.3	11.2
DeL	1	2.937	2.781	33.948	0.127	39.1	38.1-40.2	12.3	6.2
DeL	2	2.965	2.742	31.928	0.147	39.8	38.7-41.0	11.9	6.1
DeL	3	2.944	2.801	31.826	0.117	39.3	38.4-40.3	11.9	6.3
UNG	1	3.235	2.542	55.641	0.141	46.5	45.1-47.8	16.0	5.2
UNG	2	3.222	2.640	58.508	0.076	46.1	45.4-46.9	16.4	5.6
UNG	3	3.228	2.625	56.028	0.158	46.3	44.8-47.9	16.1	5.6
DeG	1	2.926	1.980	43.387	0.205	38.9	37.3-40.6	14.1	2.8
DeG	2	2.958	1.829	41.065	0.160	39.7	38.4-41.0	13.7	2.2
DeG	3	2.948	1.841	39.710	0.221	39.4	37.7-41.3	13.4	2.2

328

329 The isoelectric point (pI) of a protein indicates its relative acidity or basicity, the higher
 330 the pI, the higher the basicity of the molecule [36]. The isoelectric points (pI) of the β -
 331 galactosidase and lysozyme used are 4.6 and 11.3, respectively [13]. The molecule of β -
 332 galactosidase contains ~11 w/w% basic amino acids (histidine, lysine, and arginine) and ~22
 333 w/w% acidic (aspartic acid and glutamic acid) residues [37], i.e., approximately double the
 334 number of acidic groups compared to basic. Conversely the lysozyme used in this study contains
 335 about 18 w/w% and ~7 w/w% basic (histidine, lysine, and arginine) and acidic (aspartic acid and
 336 glutamic acid) residues, respectively [38]. [Detailed information regarding](#) the structures of β -
 337 galactosidase and lysozyme can be found in [37,38]. However, this is not the only determinant of
 338 energy as the surfaces of both the acidic (UNG) and basic (UNL) protein powders were
 339 relatively basic (the values of $\gamma_s^+ > \gamma_s^-$). Therefore to explain our results further, the interaction of
 340 protein molecules with surfaces and interfaces, during preparation using lyophilization methods,
 341 must be considered.

342 As protein molecules are surface-active, containing both polar and non-polar groups, they
343 tend to adsorb to interfaces via hydrophobic interactions (London), coulombs (electrostatic)
344 and/or hydrogen bonding, and they reorient their surfaces to the parts which give the optimum
345 attractive force and the most stable state (minimum energy) with a substrate or an interface [39].
346 Upon freezing and subsequent lyophilization, protein molecules adsorb to the formed ice via
347 hydrophobic residues confirming the mechanism proposed by Baardsnes and Davies [40]. An
348 increase in entropy drives the spontaneous interaction between the hydrophobic regions in the
349 protein molecules interact spontaneously and the ice faces [41]. The rich electron rings of
350 aromatic residues orient so that the ring structures lie flat with the interface in order to maximize
351 interaction at the interfaces and lower the Gibbs free energy of the system [42]. Therefore,
352 lyophilized protein particles expose the rich electron rings of the aromatic residues on their
353 surfaces. Aromatic groups, via their π electrons, which are considered nucleophilic, can form
354 hydrogen bonds with chemical groups (acidic polar probes) being the hydrogen donors [43].
355 Therefore, exposing these rings to surfaces relatively increases their basicity compared to their
356 acidity irrespective of the acidic or basic nature of the proteins themselves. Also, the ring
357 structures can participate in raising the dispersive surface energy via London interactions due to
358 their high polarizability [43]. The aromatic residues (tryptophan, tyrosine, and phenylalanine)
359 make up 16%w/w of the β -galactosidase molecules and 14%w/w of the lysozyme molecules
360 [37,38]. This explains the higher values of γ_s^d of β -galactosidase compared to lysozyme, prior to
361 mechanical denaturation.

362 UNG was more acidic than UNL. The size and the shape of the molecule can also
363 influence orientation. UNG is larger than UNL, with a globular shape and when chemical groups
364 are preferably exposed to a surface, (energetically or entropically) this will expose not only those

365 specific groups but also other closely associated groups which will vary in nature from one
366 protein to another. Thus, the surfaces of the acidic protein (β -galactosidase) were more acidic
367 compared to the basic protein (lysozyme).

368 Table 1 shows that mechanical denaturation decreased the dispersive free energy and the basicity
369 of the surfaces of protein powders, irrespective of the nature of the protein (acidic or basic).

370 Usually milling induces an increase in the dispersive energy due to the generation of surface
371 amorphous regions or/and creation of higher energy crystal faces because of particle
372 fracture/breakage, thus the surface acidity and basicity change according to the formation of new
373 faces and regions [44,45]. However, in our case, due to lyophilization, the protein powders are
374 amorphous with particle sizes below 5 μm . Therefore, there would be no further size reduction
375 by fracture mechanisms because of brittle ductile transition [3]. Therefore, the denatured protein
376 powders were produced by milling where the attrition mechanism was dominant and so the same
377 original faces did not change. During milling, the extensive mechanical energy completely
378 denatured the protein molecules, as confirmed by DSC and Raman results. This denaturation led
379 to aggregation of the protein molecules via non-covalent interactions through π -stacking
380 interactions [33]. This caused a loss of the aromatic groups, which are rich in π electrons, from
381 the surfaces. Therefore, a decrease in the Van der Waals interactions, a major contributor to
382 dispersive energy and nucleophilicity (basicity) occurred, and so γ_s^d and γ_s^- decreased after
383 denaturation for both proteins. Also this loss of aromatic residues from the surface of the
384 denatured powders renders γ_s^d similar for both proteins. This is further evidence that the exposed
385 aromatic residues raise the γ_s^d as outlined previously. The Raman spectroscopic results confirmed
386 that the aromatic residues were involved in the denaturation processes, therefore, supporting the
387 findings and our interpretation of the IGC studies.

388 **4. Conclusions**

389 The surface energies of the lyophilized protein powders differed according to their amino
390 acid compositions. The absence of the thermal unfolding transition phase for the proteins
391 (lysozyme and β -galactosidase) and the changes in the conformation of the back-bone and side
392 chains confirmed the mechanical milling process caused denaturation of the protein powders;
393 this could potentially be reversible in solution. The acidic protein powder (β -galactosidase) had
394 higher surface acidity (γ_s^+) and lower surface basicity (γ_s^-) compared to the basic protein powder
395 (lysozyme). However, both protein powders had relatively basic surfaces due to the rich electron
396 rings of the aromatic residues which are nucleophilic. During mechanical denaturation, these
397 rings tend to associate through π -stacking interactions and are thus concealed from the surface.
398 Their removal reduced γ_s^- and γ_s^d of the surfaces of both protein powders, and thereby yielded
399 similar γ_s^d for the surfaces of both proteins.

400

401 **Acknowledgements**

402 MAM gratefully acknowledges CARA (Stephen Wordsworth and Ryan Mundy) the Universities
403 of Bath and Bradford for providing academic fellowships.

404

405 **Supplementary data**

406 Supplementary data associated with this article can be found, in the online version, at
407 <http://dx.doi.org/XXXX>.

408

409

410

411

412

413 **References**

- 414 [1] H. Hoyer, W. Schlocker, K. Krum, A. Bernkop-Schnürch, *Eur. J. Pharm. Biopharm.* 69
415 (2008) 476.
- 416 [2] W. Schlocker, S. Gschliesser, A. Bernkop-Schnürch, *Eur. J. Pharm. Biopharm.* 62 (2006)
417 260.
- 418 [3] M.A. Mohammad, I.M. Grimsey, R.T. Forbes, *J. Pharm. Biomed. Anal.* 114 (2015) 176.
- 419 [4] W. He, K. Yang, L. Fan, Y. Lv, Z. Jin, S. Zhu, C. Qin, Y. Wang, L. Yin, *Int. J. Pharm.* 495
420 (2015) 9.
- 421 [5] R. Caillard, M. Subirade, *Int. J. Pharm.* 437 (2012) 130.
- 422 [6] V. Karde, C. Ghoroi, *Int. J. Pharm.* 475 (2014) 351.
- 423 [7] X. Han, L. Jallo, D. To, C. Ghoroi, R. Davé, *J. Pharm. Sci.* 102 (2013) 2282.
- 424 [8] D. Cline, R. Dalby, *Pharm. Res.* 19 (2002) 1274.
- 425 [9] M.S. Killian, H.M. Krebs, P. Schmuki, *Langmuir* 27 (2011) 7510.
- 426 [10] O. Planinsek, A. Trojak, S. Srcic, *Int. J. Pharm.* 221 (2001) 211.
- 427 [11] Y. Hirakura, H. Yamaguchi, M. Mizuno, H. Miyanishi, S. Ueda, S. Kitamura, *Int. J. Pharm.*
428 340 (2007) 34.
- 429 [12] Q. Husain, *Crit. Rev. Biotechnol.* 30 (2010) 41.
- 430 [13] M. Ospinal-Jiménez, D.C. Pozzo, *Langmuir* 28 (2012) 17749.
- 431 [14] R.R. Haj-Ahmad, A.A. Elkordy, C.S. Chaw, A. Moore, *Eur. J. Pharm. Sci.* 49 (2013) 519.
- 432 [15] S. Chakraborti, T. Chatterjee, P. Joshi, A. Poddar, B. Bhattacharyya, S.P. Singh, V. Gupta,
433 P. Chakrabarti, *Langmuir* 26 (2010) 3506.
- 434 [16] R.E. Hamlin, T.L. Dayton, L.E. Johnson, M.S. Johal, *Langmuir* 23 (2007) 4432.
- 435 [17] M.A. Mohammad, *J. Chromatogr. A* 1318 (2013) 270.
- 436 [18] M.A. Mohammad, *J. Chromatogr. A* 1399 (2015) 88.
- 437 [19] M.A. Mohammad, *J. Chromatogr. A* 1408 (2015) 267.
- 438 [20] B. Shi, D. Qi, *J. Chromatogr. A* 1231 (2012) 73.
- 439 [21] C. Della Volpe, D. Maniglio, M. Brugnara, S. Siboni, M. Morra, *J. Colloid Interface Sci.*
440 271 (2004) 434.
- 441 [22] S.C. Das, I. Larson, D.A. Morton, P.J. Stewart, *Langmuir* 27 (2011) 521.
- 442 [23] C.D. Volpe, S. Siboni, *J. Colloid Interface Sci.* 195 (1997) 121.
- 443 [24] J. Schultz, L. Lavielle, C. Martin, *J. Adhesion* 23 (1987) 45.
- 444 [25] C.J. Van Oss, R.J. Good, M.K. Chaudhury, *Langmuir* 4 (1988) 884.
- 445 [26] B. Maroufi, B. Ranjbar, K. Khajeh, H. Naderi-Manesh, H. Yaghoubi, *Biochim. Biophys.*
446 *Acta* 1784 (2008) 1043.
- 447 [27] J.M. Sánchez, V. Nolan, M.A. Perillo, *Colloids Surf. B Biointerfaces* 108 (2013) 1.
- 448 [28] T.J. Yu, J.L. Lippert, W.L. Peticolas, *Biopolymers* 12 (1973) 2161.
- 449 [29] E.N. Lewis, W. Qi, L.H. Kidder, S. Amin, S.M. Kenyon, S. Blake, *Molecules* 19 (2014)
450 20888.
- 451 [30] S.R. Tello-Solís, J. Jiménez-Guzmán, C. Sarabia-Leos, L. Gómez-Ruíz, A.E. Cruz-
452 Guerrero, G.M. Rodríguez-Serrano, M. García-Garibay, *J. Agric. Food Chem.* 53 (2005) 10200.
- 453 [31] P.J. Artymiuk, C.C.F. Blake, D.W. Rice, K.S. Wilson, *Acta Crystallogr. B: Struct.*
454 *Crystallogr. Cryst. Chem.* B38 (1982) 778.
- 455 [32] C. Zhou, W. Qi, E.N. Lewis, J.F. Carpenter, *Anal. Biochem.* 472 (2015) 7.
- 456 [33] S. Jang, J. Jang, W. Choe, S. Lee, *ACS Appl. Mater. Interfaces* 7 (2015) 1250.

- 457 [34] A. Torreggiani, M. Di Foggia, I. Manco, A. De Maio, S.A. Markarian, S. Bonora, J. Mol.
458 Struct. 891 (2008) 115.
- 459 [35] A. Torreggiani, M. Tamba, I. Manco, M.R. Faraone-Mennella, C. Ferreri, C. Chatgialoglu,
460 J. Mol. Struct. 744 (2005) 767.
- 461 [36] C. Sun, J.C. Berg, Adv. Colloid Interface Sci. 105 (2003) 151.
- 462 [37] Y. Tanaka, A. Kagamiishi, A. Kiuchi, T. Horiuchi, J. Biochem. 77 (1975) 241.
- 463 [38] M.C. Vaney, S. Maignan, M. Riès-Kautt, A. Ducriux, Acta Crystallogr. D. Biol. Crystallogr.
464 52 (1996) 505.
- 465 [39] C. Chaiyasut, Y. Takatsu, S. Kitagawa, T. Tsuda, Electrophoresis 22 (2001) 1267.
- 466 [40] J. Baardsnes, P.L. Davies, Biochim Biophys Acta. 160 (2002) 49.
- 467 [41] S. Pezennec, F. Gauthier, C. Alonso, F. Graner, T. Croguennec, G. Brulé, A. Renault, Food
468 Hydrocolloids 14 (2000) 463.
- 469 [42] M. Jurkiewicz-Herbich, A. Muszalska, R. Słojkowska, Colloids Surfaces A: Physicochem.
470 Eng. Aspects 131 (1998) 315.
- 471 [43] G.I. Makhatadze, P.L. Privalov, Biophys. Chem. 50 (1994) 285.
- 472 [44] U.V. Shah, Z. Wang, D. Olusanmi, A.S. Narang, M.A. Hussain, M.J. Toba, J.Y. Heng, Int.
473 J. Pharm. 495 (2015) 234.
- 474 [45] X. Han, L. Jallo, D. To, C. Ghoroi, R. Davé, J. Pharm. Sci. 102 (2013) 2282.